

LASER TREATMENT OF NIOBIUM SURFACES FOR SRF APPLICATIONS

V. Porshyn*, P. Serbun, H. Bürger, S. Soykarci, and D. Lützenkirchen-Hecht
Faculty of Mathematics and Natural Sciences, University of Wuppertal, Wuppertal, Germany

Abstract

We report on a laser surface treatment of high purity niobium (110) single crystals. Typical surface defects like scratches, pits, sharp rims and holes were eliminated by a focused pulsed ns-laser beam. A laser fluence of about 0.68 J/cm^2 and 40 - 80 pulses per spot were required to induce well detectable surface modifications. The remelted surface was sufficiently smooth, but exhibited also a number of wave structures. Thus, the surface roughness slightly increased with increasing number of pulses. Finally, boiling traces and μm -deep ablation were observed and studied as well. Local field electron emission measurements showed no emission up to 700 MV/m from a moderately remelted area below the boiling point.

INTRODUCTION

Interior surfaces of Nb cavities are nowadays treated by buffered chemical polishing (BCP) and electropolishing (EP). However, even after the polishing procedures and a surface cleaning with N_2 , high pressure rinsing with ultrapure water or dry-ice, the remaining number of surface defects and particulates that lead to parasitic field electron emission (FE) is still large, and, as a consequence, acceleration gradients of the BCP/EP treated cavities are limited to 45.5 MV/m [1]. An additional drawback of BCP/EP is a waste of a large amount of hazardous acids.

Laser polishing (LP) appears to be a promising alternative, which is feasible also for a large quantity production. It is conceivable to apply LP not only instead of BCP/EP, but also as an additional final step in the preparation of cavities. The laser beam can be easily coupled into a cavity using a motorized mirror fixed on a linear stage, which is guided along the cavity axis in such a way that any point of the interior of the cavity can be illuminated. The processing speed would depend primary on the spot size and thus on the laser fluence. In dependence on process parameters an initial surface roughness can be reduced from several tens of μm down to several hundreds of nm [2]. Furthermore, earlier studies have shown that a sufficient smoothing effect of the Nb surface is possible under pulsed ns-laser illumination [3, 4]. In general, the melting depth of Nb depends strongly on the laser fluence and can reach several hundred nm [5]. As soon as the liquefied metal starts to boil, more surface defects are produced than eliminated. Hence, the maximum laser fluence suited for a successful smoothing treatment is expected to be limited. The common approach is thus a multi-pulse illumination using a fixed laser fluence.

For our study a high purity niobium (110) single crystals with residual-resistance ratios of above 250 were used. Their initial surface roughness (R_q , root mean square

value) was 9 - 16 nm after the standard BCP/EP procedure and the high pressure rinsing with ultrapure water. After the laser treatment the surface was analysed using a scanning electron microscope (SEM, JEOL JSM-6510) and a combined system (FRT MicroProf) of an optical profilometer (OP) and an atomic force microscope (AFM). Finally, local FE measurements were performed with a FE scanning microscope (FESM) using tungsten cone needle anodes of 30 - 100 μm in diameter for typical working distance of 10 - 30 μm [6].

EXPERIMENTAL SETUP

The laser treatment was done in a vacuum chamber as shown in Fig. 1 with a pressure around $4 \times 10^{-6} \text{ Pa}$. The sample was positioned on a rod in the middle of the chamber, applying a perpendicular illumination by a pulsed Nd:YAG laser (EKSPLA NT342A-SH) with a pulse duration of 3.5 ns, wavelength of 355 nm and repetition rate of 10 Hz. The spot position on the sample and the spot size was set by moving and tilting a focusing lens (focal length 75 mm). The typical spot exhibited a Gaussian profile with $1/e^2$ -width of ca. 210 μm . Basically the sample holder was separated from the ground, thus electrical signals induced during the illumination process could be measured as well.

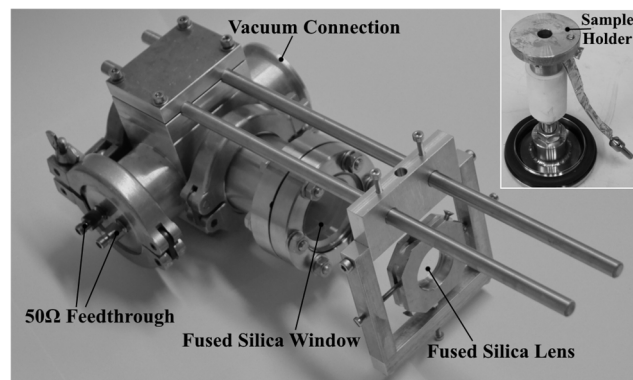


Figure 1: Overview photo of the vacuum chamber used in the experiment. The inset shows the inner part of the system, in particular the sample holder.

RESULTS

Transition from Laser Melting to Laser Ablation

In the following, the samples were exposed to a focused laser beam at different positions, see Fig. 2. The applied laser fluence (F) at the surface was in the range from ca. 0.68 J/cm^2 to ca. 4.27 J/cm^2 and the number of pulses (N) on each spot was varied from 20 to 200 pulses.

A remarkable surface melting occurred for laser fluences of above 0.68 J/cm^2 and at least 40 pulses, see inset 1 of Fig. 2. Moreover, as shown in the inset 2 of Fig. 2, pronounced pinholes and cavities appeared in the illuminated

* porshyn@uni-wuppertal.de

Any distribution of this work must maintain attribution to the author(s), title of the work, publisher, and DOI.

area for the following parameters: $F = 1.4 \text{ J/cm}^2$, $N = 80$; $F = 2.07 \text{ J/cm}^2$, $N = 60$; $F = 2.89 \text{ J/cm}^2$, $N = 40$; $F = 3.53 \text{ J/cm}^2$, $N = 20$. These features were most likely to be caused by vapour bubbles that appear during the boiling [7]. A further increase of laser power and number of pulses resulted in a significant irregular removal of material leading to μm -deep craters with μm -high edges, see inset 3 of Fig. 2. Remarkably, the occurrence of the destructive laser ablation was actually not expected at all for laser fluences below 5 J/cm^2 [7]. Hence, the repetition rate of 10 Hz was obviously too high for the illuminated surface to calm down between the pulses.

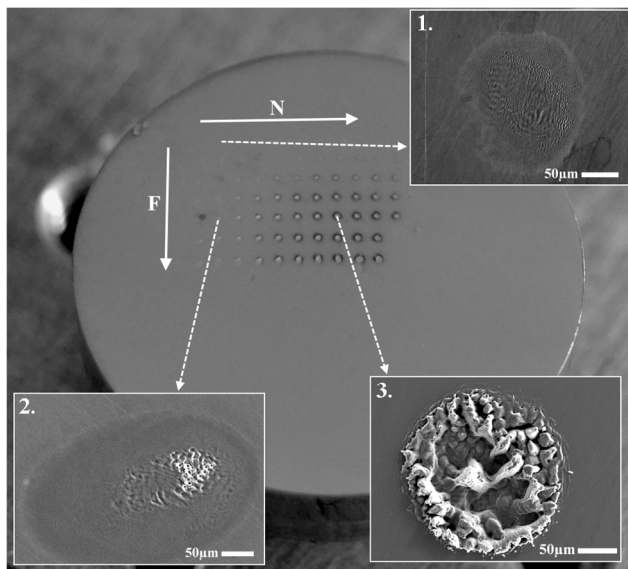


Figure 2: Nb sample after the laser treatment at different places with increasing laser fluence, F , and pulse number, N , as indicated by the corresponding arrows. The insets present the spot shapes measured with SEM for (1) $F = 0.68 \text{ J/cm}^2$, $N = 40$; (2) $F = 2.89 \text{ J/cm}^2$, $N = 40$; and (3) $F = 2.89 \text{ J/cm}^2$, $N = 160$.

Smoothing Effect of Laser Treatment

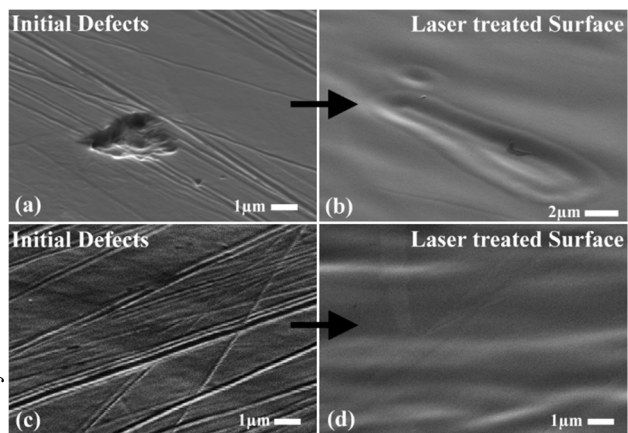


Figure 3: (a) and (c) SEM micrographs of several representative surface defects prior to laser illumination. (b) and (d) represent typical smoothed regions after laser illumination with $F = 0.68 \text{ J/cm}^2$, $N = 120$.

No boiling traces were observed in the experiment for a laser fluence of 0.68 J/cm^2 and maximum applied pulse number up to 200. Typical sharp surface defects like scratches and holes could be efficiently eliminated due to the melting at this fluence level as demonstrated in Fig. 3.

Surface Roughness and Laser-Induced Defects

The surface topography of remelted regions, which exhibited no boiling traces, was analysed in terms of R_q and the power spectral density (PSD). The behavior of R_q for representative segments ($50 \times 50 \mu\text{m}^2$) of the illuminated area with the corresponding initial roughness is presented in Fig. 4a. It follows that the overall roughness was more sensitive to the laser fluence than to the total number of pulses. The maximum measured roughness ($R_{q,\text{max}}$) for $F = 0.68 \text{ J/cm}^2$ was around 50 nm , thus slightly higher than the initial value of ca. 20 nm . Moreover, a kind of saturation above $N = 140$ for the magnitude of laser induced defects can be suggested. On the other hand, $R_{q,\text{max}}$ of ca. 190 nm and 140 nm was measured for $F = 1.4 \text{ J/cm}^2$ and $F = 2.07 \text{ J/cm}^2$, respectively. Hence, despite a positive effect of the surface smoothing, a higher laser fluence systematically led to a significant increase of roughness and laser-induced defects.

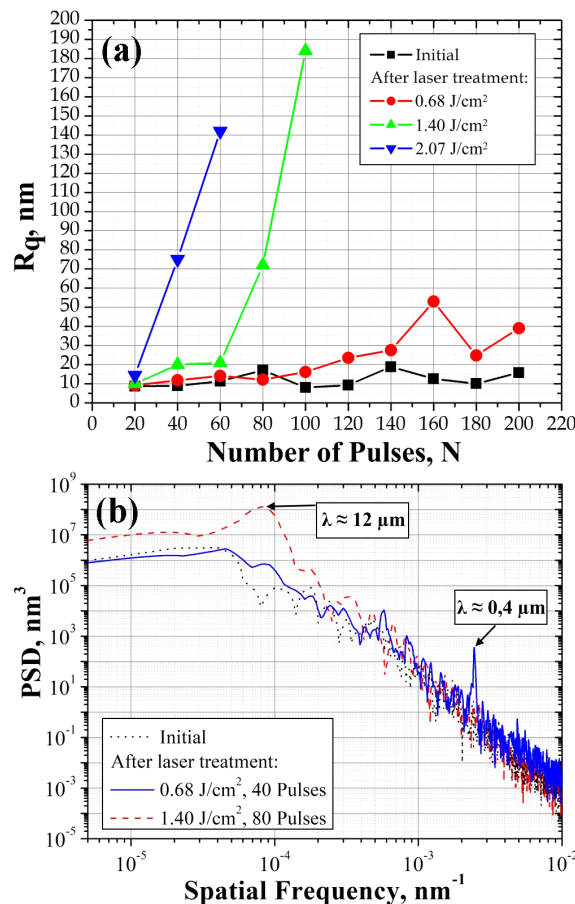


Figure 4: Surface roughness, R_q , vs. number of pulses, N , for different values of the laser fluence as measured with AFM in (a). Here the initial roughness of the illuminated regions is presented as well. (b) PSD plot of the initial surface in comparison to the laser treated surface.

The peaks in the PSD analysis at about $0.4 \mu\text{m}$ and $12 \mu\text{m}$ in Fig. 4b suggest that typical laser-induced defects were wave structures. Two different kinds of them could be identified as described further.

Fringes with a distance of around 400 nm to each other dominated for a low laser fluence and a small number of pulses, see Fig. 5a. They were also observed at the boundaries of the melted spots. This kind of wave structures is known to result from an interference of the incident, linearly polarised laser beam with electromagnetic waves scattered at the surfaces [8]. So in general, the distance between the fringes in this case depends on the laser wavelength and its incident angle on the surface. Moreover, the fringes run typically perpendicular to the polarization of the laser beam.

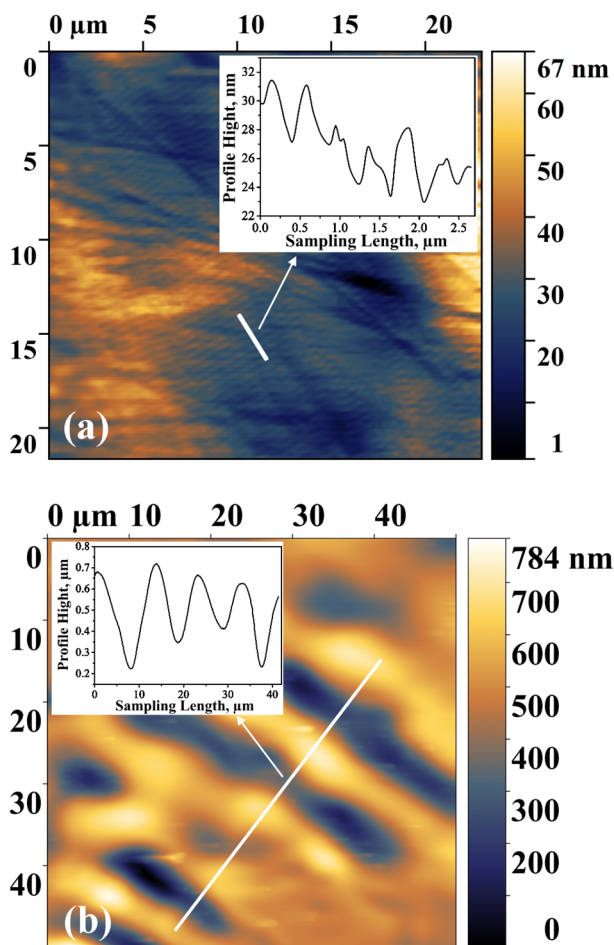


Figure 5: AFM micrographs of laser treated areas for (a) $F = 0.68 \text{ J/cm}^2$, $N = 40$ in and (b) $F = 1.4 \text{ J/cm}^2$, $N = 80$. Insets show profiles along the propagation direction of the outstanding wave structures as described in the text.

Different wave structures were created in particular at the middle part of the melted spots and appeared rather in the form of circular fringes. They exhibited wavelengths of around $10 \mu\text{m}$ and contributed significantly to the overall surface roughness, see Fig. 5b. Our assumption is that their shape possibly reflects a behavior of a liquefied metal in terms of periodic pressure fluctuations, which occur directly after the laser illumination.

Field Emission from Laser Smoothed Surface

Two local FE studies are exemplarily presented in Fig. 6, i. e. one was carried out for an initial surface with typical defects as shown in Fig. 3a and the other for the laser treated surface with $F = 0.68 \text{ J/cm}^2$, $N = 200$, e. g. see inset 1 of Fig. 2. In both cases an erratic activation of emitting structures was observed during the up cycle as far as the emission current raised to several pA. Then a reduced FE-threshold resulted for the down cycle. Furthermore, additional craters appeared in the investigated areas, which hinted on an explosive break down, i. e. an explosive electron emission [9]. Remarkably, the FE-threshold for the laser treated spot before the break down was found to be around 750 MV/m in spite of the above discussed wave structures, and thus significantly higher in comparison to the value of ca. 150 MV/m for the untreated surface with a typical surface defect (see Fig. 3a). A more detailed analysis of the I-E-curves and a possible correlation and modelling between the processing parameters and FE-behavior is ongoing.

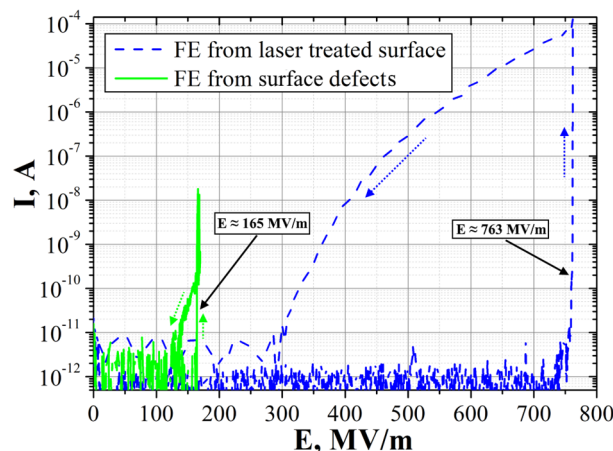


Figure 6: Cathode current, I , vs. macroscopic electrical field, E , for laser treated ($F = 0.68 \text{ J/cm}^2$, $N = 200$) and untreated surfaces. The dotted arrows emphasize the voltage cycle applied to the cathode.

CONCLUSION

Local LP of niobium (110) single crystals was realised for laser fluences of around 0.68 J/cm^2 . Sharp surface defects, which could not be removed by electropolishing and other methods, were efficiently smoothed by the laser illumination. In dependence on the processing parameters, i. e. F and N , the laser treatment induced different wave-like structures with magnitudes up to several hundreds of nm. Nevertheless, the laser treated surface exhibited rather high FE breakdown thresholds of up to 750 MV/m . Thus, LP appears to be a very promising polishing technique for the further improvement of interior surfaces of superconductive cavities.

ACKNOWLEDGEMENT

The research was funded by the German Federal Ministry of Education and Research under project number 05H15PXR1.

REFERENCES

- [1] W. Singer, X. Singer, A. Brinkmann, J. Iversen, A. Matheisen, A. Navitski, Y. Tamashevich, P. Michelato, and L. Monaco, *Supercond. Sci. Technol.*, Vol. 28, p. 085014, 2015.
- [2] B. Rosa, P. Mognol, and J. Hascoët, *J. Laser Appl.*, vol. 27, p. S29102, 2015.
- [3] L. Zhao, J.M. Klopff, C.E. Reece, and M.J. Kelley, *Phys. Rev. Spec. Top. Accel. Beams*, vol. 17, p. 083502, 2014.
- [4] L. Zhao, J.M. Klopff, C.E. Reece, and M.J. Kelley, *Materialwiss. Werkstofftech.*, vol. 46, p. 675, 2015.
- [5] N.M. Bulgakova, A.V. Bulgakov, and L.P. Babich, *Appl. Phys. A*, vol. 79, p. 1323, 2004.
- [6] D. Lysenkov and G. Müller, *Int. J. Nanotechnology*, vol. 2, p. 239, 2005.
- [7] N.M. Bulgakova and A.V. Bulgakov, *Appl. Phys. A*, vol. 73, p. 199, 2001.
- [8] J.F. Young, J.S. Preston, H.M. van Driel, and J.E. Sipe, *Phys. Rev. B*, vol. 27, p. 1155, 1983.
- [9] G. A. Mesyats, *Plasma Phys. Controlled Fusion*, vol. 47, p. A109, 2005.

Content from this work may be used under the terms of the CC BY 3.0 licence (© 2018). Any distribution of this work must maintain attribution to the author(s), title of the work, publisher, and DOI.